

formation cannot occur in systems in which all diffusion coefficients are equal. [For a comprehensive discussion of these issues, see Pearson and co-workers (10, 11); for a discussion of Turing instabilities in the model at hand, see Vastano *et al.* (12).] The only Turing patterns that can occur bifurcate off the nontrivial steady uniform state (the blue state). Most of the patterns discussed in this report occur for parameter values such that the nontrivial steady state does not exist. With the ratio of diffusion coefficients used here, Turing patterns occur only in a narrow parameter region in the vicinity of  $F = k = 0.0625$ , where the line of saddle-node bifurcations coalesces with the line of Hopf bifurcations. In the vicinity of this point, the branch of small-amplitude Turing patterns is unstable (12).

With equal diffusion coefficients, no patterns formed in which small asymmetries in the initial conditions were amplified by the dynamics. This observation can probably be understood in terms of the following fact: Nonlinear plane waves in two dimensions cannot be destabilized by diffusion in the case that all diffusion coefficients are equal (13). During the initial stages of the evolution, the corners of the square perturbation are rounded off. The perturbation then evolves as a radial wave, either inward or outward depending on the parameter values. Such a wave cannot undergo spontaneous symmetry breaking unless the diffusion coefficients are unequal. However, I found symmetry breaking over a wide range of parameter values for a ratio of diffusion coefficients of 2. Such a ratio is physically reasonable even for small molecules in aqueous solution. Given this diffusion ratio and the wide range of parameters over which the replicating spot patterns exist, it is likely that they will soon be observed experimentally.

Recently Hasslacher *et al.* have demonstrated the plausibility of subcellular chemical patterns through lattice-gas simulations of the Selkov model (14). The patterns discussed in the present article can also be found in lattice-gas simulations of the Selkov model and in simulations carried out in three space dimensions. Perhaps they are related to dynamical processes in the cell such as centrosome replication.

## REFERENCES AND NOTES

1. G. Nicolis and I. Prigogine, *Self-Organization in Non-Equilibrium Systems* (Wiley, New York, 1977).
2. E. E. Selkov, *Eur. J. Biochem.* **4**, 79 (1968).
3. P. Gray and S. K. Scott, *Chem. Eng. Sci.* **38**, 29 (1983); *ibid.* **39**, 1087 (1984); *J. Phys. Chem.* **89**, 22 (1985).
4. J. A. Vastano, J. E. Pearson, W. Horsthemke, H. L. Swinney, *Phys. Lett. A* **124**, 6 (1987). *ibid.*, p. 7; *ibid.*, p. 320.
5. K. J. Lee, W. D. McCormick, Q. Ouyang, H. L. Swinney, *Science* **261**, 192 (1993).
6. P. Hohenberg and M. Cross, *Rev. Mod. Phys.* **65**, 3 (1993).

7. J. Guckenheimer and P. Holmes, *Nonlinear Oscillations, Dynamical Systems, and Bifurcations of Vector Fields* (Springer-Verlag, Berlin, 1983), chap. 3.
8. Y. Kuramoto, *Chemical Oscillations, Waves, and Turbulence* (Springer-Verlag, Berlin, 1984).
9. A. Kawczynski, W. Comstock, R. Field, *Physica D* **54**, 220 (1992); A. Hagberg and E. Meron, University of Arizona preprint.
10. J. E. Pearson and W. Horsthemke, *J. Chem. Phys.* **90**, 1588 (1989).
11. J. E. Pearson and W. J. Bruno, *Chaos* **2**, 4 (1992); *ibid.*, p. 513.
12. J. A. Vastano, J. E. Pearson, W. Horsthemke, H. L. Swinney, *J. Chem. Phys.* **88**, 6175 (1988).
13. J. E. Pearson, *Los Alamos Publ. LAUR 93-1758* (Los Alamos National Laboratory, Los Alamos, NM, 1993).
14. B. Hasslacher, R. Kapral, A. Lawniczak, *Chaos* **3**, 1 (1993).
15. I am happy to acknowledge useful conversations with S. Ponce-Dawson, W. Horsthemke, K. Lee, L. Segel, H. Swinney, B. Reynolds, and J. Theiler. I also thank the Los Alamos Advanced Computing Laboratory for the use of the Connection Machine and A. Chapman, C. Hansen, and P. Hinker for their ever-cheerful assistance with the figures.

7 April 1993; accepted 13 May 1993

## Pattern Formation by Interacting Chemical Fronts

Kyoung J. Lee, W. D. McCormick, Qi Ouyang, Harry L. Swinney\*

Experiments on a bistable chemical reaction in a continuously fed thin gel layer reveal a new type of spatiotemporal pattern, one in which fronts propagate at a constant speed until they reach a critical separation (typically 0.4 millimeter) and stop. The resulting asymptotic state is a highly irregular stationary pattern that contrasts with the regular patterns such as hexagons, squares, and stripes that have been observed in many nonequilibrium systems. The observed patterns are initiated by a finite amplitude perturbation rather than through spontaneous symmetry breaking.

In recent years, pattern formation has become a very active area of research, motivated in part by the realization that there are many common aspects of patterns formed by diverse physical, chemical, and biological systems and by cellular automata and differential equation models. In experiments on a chemical system, we have discovered a new type of pattern that differs qualitatively from the previously studied chemical waves [rotating spirals (1)], stationary "Turing" patterns (2–4), and chaotic patterns (5). These new patterns form only in response to large-amplitude perturbations—small-amplitude perturbations decay. A large perturbation evolves into an irregular pattern that is stationary (time-independent) (Fig. 1). The patterns have a length scale determined by the interaction of the chemical fronts, which propagate toward one another at constant speed until they reach a critical distance and stop, as Fig. 2 illustrates. The growth of these front patterns is markedly different from Turing patterns: The front patterns develop locally and spread to fill space, as in crystal growth, whereas Turing patterns emerge spontaneously everywhere when the critical value of a control parameter is exceeded.

The front patterns are highly irregular, in contrast with Turing patterns, which emerge as a regular array of stripes or hexagons (in two-dimensional systems) at the

transition from a uniform state (4). The interaction of fronts illustrated in Fig. 2 also contrasts with the behavior in excitable chemical media, where colliding fronts annihilate one another (1), and with solitons, where nonlinear waves pass through one another (6).

Our experiments have been conducted using an iodate-ferrocyanide-sulfite reaction, which is known to exhibit bistability and large oscillations in pH in stirred flow reactors (7). The other reactions that yield stationary chemical patterns are the well-studied chlorite-iodide-malonic acid reaction (3–5) and a variant reaction (8) that uses chlorine dioxide instead of chlorite. We chose the iodate-ferrocyanide-sulfite reaction as a new candidate for studies of pattern formation because a pH indicator could be used to visualize patterns that might form.

The following experiments illustrate the differences between our patterns and those previously observed in reaction-diffusion systems. A diagram of the gel disc reactor is shown in Fig. 3. Gel-filled reactors were developed several years ago (9) to study reaction-diffusion systems maintained in well-defined states far from equilibrium. These reactors are now widely used for studying sustained patterns that arise solely from the interplay of diffusion and chemical kinetics—the gel prevents convective motion. A thin polyacrylamide gel layer (0.2 mm thick, 22 mm in diameter) is fed diffusively by a continuously refreshed reservoir of chemicals (10). There are two thin membranes between the polyacrylamide

Center for Nonlinear Dynamics and the Department of Physics, University of Texas at Austin, Austin, TX 78712.

\*To whom correspondence should be addressed.

ide gel and the stirred reservoir, one (an Anopore disk, 0.06 mm thick with 0.2- $\mu$ m-diameter pores) that provides structural rigidity for the thin gel layer and another (a nitrocellulose membrane, 0.14 mm thick with 0.45- $\mu$ m-diameter pores) that provides a white backing for visualization of the patterns. The chemicals are premixed (in a 0.5-ml cell) before entering the reactor reservoir (2.5 ml), and the reservoir is vigorously stirred to ensure homogeneity. The concentrations of the feed chemicals are held fixed at the values given in the caption for Fig. 3; only the flow rate is varied. The reagent concentrations in the reservoir are time-independent at each flow rate throughout the range studied. In the flow rate range in which patterns are observed, the reservoir pH increases only slightly, from 7.24 to 7.32; the fluctuations in pH are less than 0.01 at each flow rate. Patterns are observed in reflected light with a video camera connected to a digitizing board in a microcomputer.

The same type of patterns form both with and without a pH indicator: Fig. 4A was obtained with bromothymol blue indicator (which changes from yellow to blue as pH increases from 6.0 to 7.6), and Fig. 4B was obtained without an indicator (11). We examined patterns without an indicator after observing that the reaction in a stirred flow reactor exhibits large oscillations in the optical absorption band from 410 to 430 nm, where ferrocyanide absorbs strongly. The patterns observed without an indicator (with illumination at  $420 \pm 20$  nm) have higher contrast than the patterns observed with bromothymol blue indicator (with illumination at  $620 \pm 10$  nm), as can be seen by comparing Figs. 4A and 4B.

The structure of a pattern is clearer when plotted in a binary form with intensities above an arbitrary threshold in white and intensities below the threshold in

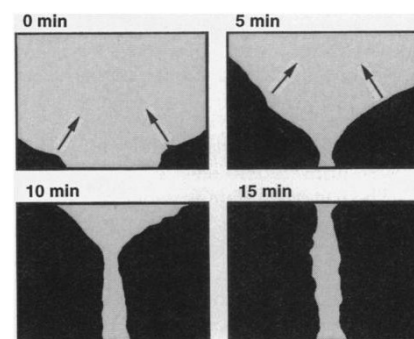
black, as can be seen by comparing the binary image in Fig. 4C with the original gray-scale data in Fig. 4B. (For clarity, the other figures in this report are shown in binary form.)

The bifurcation diagram in Fig. 5A shows the ranges of flow rate  $F$  for stable, uniform states at low and high pH and the patterned state. No patterns form in the absence of a perturbation. If the system is initially in the uniform low pH state and  $F$  is slowly increased, the system remains in the low pH state until  $F = F_{LH}$ , where there is a spontaneous transition to the uniform high pH state. (Subscripts L, H, and P correspond to low, high, and pattern.) Similarly, if  $F$  is slowly decreased from a large value, the system remains in the high pH state until  $F = F_{HL}$ , where there is a spontaneous transition to the uniform low pH state.

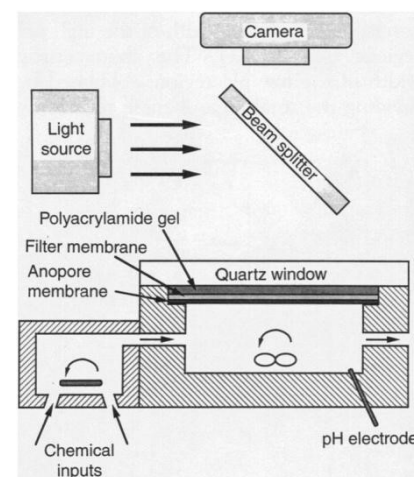
Light can be used to perturb the system because the chemistry is photosensitive. Patterns can be initiated by illuminating the system with ultraviolet light when  $F$  is between  $F_{LP}$  and  $F_{PH}$ . If the low pH state is illuminated with intense ultraviolet light (for example, for 5 min with 254-nm radiation from a 100-W Hg lamp), the illuminated region becomes dark, corresponding to the high pH state. If the illumination is uniform, the system makes a transition from the low pH state to the high pH state and remains in the high pH state after the perturbation is removed. If the illumination is local and  $F$  is in the interval  $(F_{LP}, F_{PH})$ , then removal of the perturbation results in growth of the dark spot (after an initial decay) and evolution into an irregular pattern, as Fig. 1 illustrates. This asymptotic state is independent of both the duration and the intensity of the illumination as long as a threshold is exceeded. Pattern growth usually initiates near an edge of the disc but sometimes occurs in the middle. Patterns

can be initiated with a large-amplitude ultraviolet light perturbation for flow rates up to  $F_{PH}$ ; for  $F > F_{PH}$  the system spontaneously makes a transition from a pattern to the uniform high pH state. Patterns sometimes form even without perturbation if the system is abruptly changed to be in the region  $F_{LP} < F < F_{PH}$ . In this case, the medium initially appears to be excitable, but the wave interaction illustrated in Fig. 2 results in asymptotic irregular patterns.

The disappearance of the patterns after an increase of  $F$  above a critical value  $F_{PH}$  is quite striking, as Fig. 6 illustrates. Rather

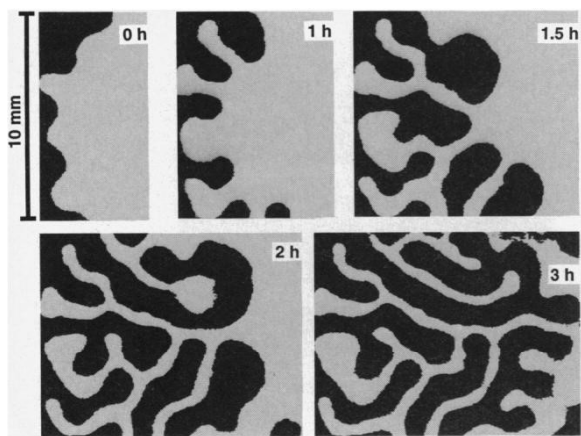


**Fig. 2.** Time evolution of two approaching chemical fronts. The fronts stop when the separation is  $\sim 0.4$  mm. This figure is a close-up view of a small region in Fig. 1 (flow rate, 131 ml/hour).



**Fig. 3.** Schematic diagram of the gel reactor and optical system. The reactor is drawn to scale except that the thicknesses of the gel, filter membrane, and Anopore membrane are four times larger than scale size. Input chemical concentrations:  $[\text{NaIO}_3] = 75.0$  mM;  $[\text{Na}_2\text{SO}_3] = 89.0$  mM;  $[\text{K}_4\text{Fe}(\text{CN})_6 \cdot 3\text{H}_2\text{O}] = 25.0$  mM;  $[\text{H}_2\text{SO}_4] = 4.5$  mM;  $[\text{NaOH}] = 0.25$  mM; and (in experiments in which a pH indicator was used)  $[\text{bromothymol blue}] = 0.15$  mM. The reactor temperature was  $30.0^\circ \pm 0.1^\circ\text{C}$ .

**Fig. 1.** Time evolution of a pattern initiated by a perturbation with intense ultraviolet light at the left boundary. The pattern achieved 3 hours (3 h) after the localized perturbation is removed was essentially stationary. (A subsequent slow evolution, perhaps due to a slow drift in feed conditions, occurs on the time scale of days.) The pattern was visualized with bromothymol blue pH indicator; white regions correspond to low pH and black regions to high pH. Chemical concentrations are given in the caption for Fig. 3; reservoir flow rate, 130 ml/hour.



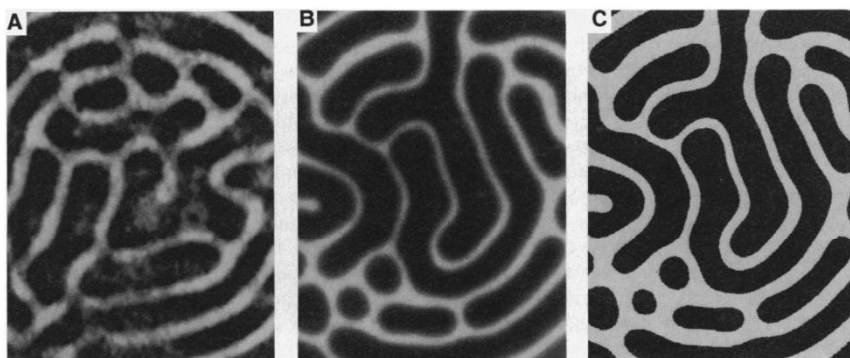


**Fig. 4.** Time asymptotic patterns obtained (A) with a pH indicator (flow rate, 127 ml/hour) and (B) without a pH indicator (flow rate, 130 ml/hour). Dark regions correspond to low ferrocyanide concentration and light regions to high ferrocyanide concentration. The patterns in (A) and (B) are shown with 256 levels of gray scale. The pattern in (B) is rendered in (C) in black and white with an arbitrarily chosen threshold. The domain shown is 10 mm by 13 mm.

than shrinking in width, the white lines slowly shrink to zero length.

The patterned state is stable for  $F$  down to  $F_{PL}$ . The hysteresis in the range  $F_{PL} < F < F_{LP}$  can be seen in Fig. 5A (12). The transition sequence in Fig. 5A was observed by using the bromothymol blue indicator, but the same sequence was observed without the indicator (13). The same type of behavior was also observed with an agar rather than a polyacrylamide gel, but agar was not used for detailed measurements because the gel degrades in a few hours.

The patterns have a characteristic length scale corresponding to the width of the low pH regions and a larger length scale corresponding to the width of the high pH regions (see Fig. 1). The characteristic width of the low pH regions, obtained by dividing the total area of these regions by

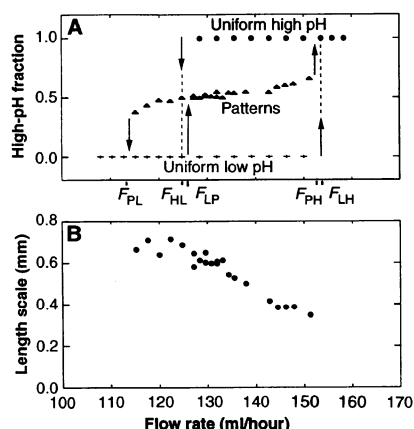


**Fig. 5.** Diagram showing transitions to and from the patterned state and to and from the uniform low pH and high pH states. (A) Fractional size of the high pH (black) region of the pattern. (B) A characteristic length scale obtained by dividing the area of the low pH (white) domain by one-half its perimeter.

the length of the perimeter around the regions, is comparable to the width of a front. This length decreases with increasing flow rate, as Fig. 5B illustrates, whereas the length scale of the high pH regions increases slowly with flow rate. The pattern readjusts after each change in flow rate. No hysteresis in the length scales was observed in measurements made with increasing and decreasing  $F$ . Although the patterns have two well-defined characteristic length scales, they are always irregular, in contrast to Turing patterns which form regular arrays of hexagons or stripes (3, 4).

A numerical analysis of a one-dimensional model system with Gray-Scott kinetics has demonstrated that stationary patterns can form in response to a finite amplitude perturbation in a system with equal diffusion coefficients (14), whereas Turing patterns form only with an appropriate inequality of diffusion coefficients (15). We do not know if inequality of

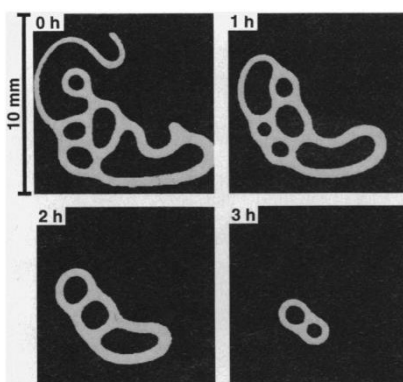


**Fig. 6.** Disappearance of a pattern following an increase of flow rate beyond a critical value,  $F_{PH}$ . At time  $t = 0$ , the flow rate was changed from 144 to 149 ml/hour. These experiments were conducted without a pH indicator.

diffusion coefficients plays a significant role in our patterns, but we note that the diffusion coefficient for the hydrogen ions is several times greater than that of the other species in the reaction.

The front patterns that we have observed originate from the interplay between reaction and diffusion and have a characteristic length scale determined not by the geometry but by the diffusion coefficients and chemical kinetics, just as is the case for spiral patterns and Turing patterns. However, the interaction of propagating fronts in our patterns is strikingly different from that observed in previous studies of reaction-diffusion systems. The necessary conditions for the formation of these front patterns have not been established, but it seems likely that such patterns will form in many bistable systems.

## REFERENCES AND NOTES

1. A. N. Zaikin and A. M. Zhabotinskii, *Nature* **225**, 535 (1970); A. T. Winfree, *Science* **175**, 634 (1972); J. Maselko and K. Showalter, *Nature* **339**, 22 (1989).
2. A. M. Turing, *Philos. Trans. R. Soc. London Ser. B* **237**, 37 (1952).
3. V. Castets, E. Dulos, J. Boissonade, P. De Kepper, *Phys. Rev. Lett.* **64**, 2953 (1990).
4. Q. Ouyang and H. L. Swinney, *Nature* **352**, 610 (1991).
5. ———, *Chaos* **1**, 4 (1991).
6. P. G. Drazin and R. S. John, *Solitons: An Introduction* (Cambridge Univ. Press, Cambridge, 1989).
7. E. C. Edblom, M. Orbán, I. R. Epstein, *J. Am. Chem. Soc.* **108**, 2826 (1986); V. Gáspár and K. Showalter, *ibid.* **109**, 4869 (1987); *J. Phys. Chem.* **94**, 4973 (1990).
8. I. R. Epstein, I. Lengyel, S. Kádár, M. Kagan, M. Yokoyama, *Physica A* **188**, 26 (1992).
9. Z. Noszticzius, W. Horsthemke, W. D. McCormick, H. L. Swinney, W. Y. Tam, *Nature* **329**, 619 (1987); W. Y. Tam, W. Horsthemke, Z. Noszticzius, H. L. Swinney, *J. Chem. Phys.* **88**, 3395 (1988).
10. The gel is sufficiently thin so that the patterns can be considered approximately two-dimensional, but we cannot rule out some three-dimensional effects arising from the finite thickness of the gel. The preparation of the gel is described in K. J. Lee, W. D. McCormick, Z. Noszticzius, H. L. Swinney, *J. Chem. Phys.* **96**, 5 (1992).
11. Black and white are reversed in the pictures obtained without an indicator so that the low pH state is white in all figures.
12. It may be possible to have hysteresis at the high flow rate end as well as the low flow rate end of the range in which patterns form, but we have not tested for this hysteresis because we have not found a perturbation method to create low pH domains in the high pH state.
13. With an indicator the values for  $F_{PL}$ ,  $F_{HL}$ ,  $F_{LP}$ ,  $F_{PH}$ , and  $F_{LH}$  are 115, 125, 126, 152, and 154 ml/hour, respectively; without an indicator the values shift upward a few percent except for  $F_{PH}$ , which shifts downward 5%.
14. J. A. Vastano, J. E. Pearson, W. Horsthemke, H. L. Swinney, *Phys. Lett. A* **124**, 7 (1987).
15. J. Pearson and W. Horsthemke, *J. Chem. Phys.* **90**, 3 (1989); I. Lengyel and I. R. Epstein, *Science* **251**, 650 (1991); J. E. Pearson and W. Bruno, *Chaos* **2**, 513 (1992).
16. We thank J. Pearson and D. Vigil for helpful discussions. This research is supported by the Department of Energy Office of Basic Energy Sciences and the Robert A. Welch Foundation.

31 March 1993; accepted 13 May 1993